SEE COMMENTARY

The role of PI3K/AKT-related PIP5K1α and the discovery of its selective inhibitor for treatment of advanced prostate cancer

Julius Semenas[a], Andreas Hedblom[a,1], Regina R. Miftakhova[a,1], Martuza Sarwar[a,1], Rikard Larsson[b,1], Liliya Shcherbina[a,c,1], Martin E. Johansson[d], Pirkko Härkönen[e], Olov Sterner[b], and Jenny L. Persson[a,2]

[a]Division of Experimental Cancer Research, Department of Laboratory Medicine, Clinical Research Center, [c]Division of Neuroendocrine Cell Biology, Department of Clinical Science, Clinical Research Center, and [d]Department of Laboratory Medicine, Lund University, 20502, Malmö, Sweden; [b]Center for Analysis and Synthesis, Lund University, 22100, Lund, Sweden; and [e]Institute of Biomedicine, Department of Cell Biology and Anatomy, University of Turku, 20520 Turku, Finland

Edited by Owen N. Witte, Howard Hughes Medical Institute, University of California, Los Angeles, CA, and approved July 3, 2014 (received for review April 1, 2014)

Nitrogen-containing heterocyclic compounds are an important class of molecules that are commonly used for the synthesis of candidate drugs. Phosphatidylinositol-4-phosphate 5-kinase-α (PIP5Kα) is a lipid kinase, similar to PI3K. However, the role of PIP5K1α in oncogenic processes and the development of inhibitors that selectively target PIP5K1α have not been reported. In the present study we report that overexpression of PIP5K1α is associated with poor prognosis in prostate cancer and correlates with an elevated level of the androgen receptor. Overexpression of PIP5K1α in PNT1A nonmalignant cells results in an increased AKT activity and an increased survival, as well as invasive malignant phenotype, whereas siRNA-mediated knockdown of PIP5K1α in aggressive PC-3 cells leads to a reduced AKT activity and an inhibition in tumor growth in xenograft mice. We further report a previously unidentified role for PIP5K1α as a druggable target for our newly developed compound ISA-2011B using a high-throughput KINOMEscan platform. ISA-2011B was discovered during our synthetic studies of C-1 indol-3-yl substituted 1,2,3,4-tetrahydroisoquinolines via a Pictet-Spengler approach. ISA-2011B significantly inhibits growth of tumor cells in xenograft mice, and we show that this is mediated by targeting PIP5K1α-associated PI3K/AKT and the downstream survival, proliferation, and invasion pathways. Further, siRNA-mediated knockdown of PIP5K1α exerts similar effects on PC3 cells as ISA-2011B treatment, significantly inhibiting AKT activity, increasing apoptosis and reducing invasion. Thus, PIP5K1α has high potential as a drug target, and compound ISA-2011B is interesting for further development of targeted cancer therapy.

cancer metastasis | drug discovery | kinase inhibitor | targeted therapy

The mainstay of cancer treatment largely consists of nonspecific cytotoxic agents with severe side effects in treated cancer patients (1). It is thus essential to discover novel drugs and their targets to more selectively eradicate cancer cells. Within the pharmaceutically important heterocyclic compounds, the 1,2,3,4-tetrahydroquinoline and 1,2,3,4-tetrahydroisoquinoline ring systems are common structural motifs found in several biologically active compounds (2–6). The discovery and development of a novel class of 1,2,3,4-tetrahydroisoquinoline derivatives as selective anticancer drugs represent new challenges in the discovery and development of anticancer drugs.

The phosphoinositide family of lipids consists of several derivatives of phosphatidylinositols (PtdIns) that are formed through a series of phosphorylation by enzymes termed phosphatidylinositol-phosphate kinases (PIPKs) (7). Among the PIPKs, PI3Ks are the best-characterized enzymes that commonly are targets for anticancer drugs (8). Less is known about PI-4-phosphate 5 kinases (PIP5Ks), enzymes that are upstream of PI3K (9, 10). The PIP5K family of lipid kinases consists of the three isozymes α, β, and γ (11–13). PIP5K1α is located in the chromosomal region 1q21.3 (14), the product of which is predominantly responsible for the synthesis of PtdIns-4,5-P_2 (PIP2), a substrate used by PI3K to produce PtdIns-3,4,5-P_3 (PIP3) (15). PIP3 in turn activates the AKT family of serine/threonine kinases (16, 17). The aberrant activation of AKT is one of the most frequently observed alterations in human cancer cells, and an elevated level of phosphorylated AKT at Ser-473 site (pSer-473) is associated with mutations in *PIK3CA (p110α)*, a PI3K subunit, or in phosphatase and tensin homolog *(PTEN)* gene in metastatic cancers (18, 19). In prostate cancer (PCa), PI3K/AKT has been reported to cross-activate androgen receptor (AR)-mediated signaling to promote progression of castration-resistant PCa (20–24). AR signaling has also been used as a target for designing drugs to treat lethal metastatic PCa (24–28).

Given the fact that PIP5K1α produces PIP2, which is required for the activation of PI3K/AKT, we anticipate that PIP5K1α may play an important role in cancer progression. It is of importance to investigate whether PIP5K1α may be used as a potential target for developing effective novel anticancer drugs. It is known that PIP5K1α is expressed at low levels in lipid tissues and is dispensable during organ development, because deletion of PIP5K1α does not result in lethal defects in mice but causes impaired spermatogenesis in males (29, 30). A recently reported study shows that PIP5K1α is highly expressed in the human MDA-MB-231

Significance

Prostate cancer is the most common malignancy and the third leading cancer-related cause of death among men of the Western world. Treatment options at advanced stages of the disease are scarce, and better therapies are in urgent need. In our study, we show that the clinically relevant lipid kinase phosphatidylinositol-4-phosphate 5-kinase-α (PIP5Kα) plays an important role in cancer cell invasion and survival by regulating the PI3K/AKT/androgen receptor pathways. Elevated levels of PIP5K1α contribute to cancer cell proliferation, survival, and invasion. In this context we introduce a newly developed compound, ISA-2011B, with promising anticancer effects by inhibiting the PIP5K1α-associated AKT pathways. Conclusively, we propose that PIP5K1α may be used as a potential therapeutic target for treatment of advanced prostate cancer.

Author contributions: J.S., A.H., R.R.M., M.S., R.L., L.S., M.E.J., P.H., O.S., and J.L.P. designed research; J.S., A.H., R.R.M., M.S., R.L., and L.S. performed research; P.H., O.S., and J.L.P. contributed new reagents/analytic tools; J.S., A.H., R.R.M., M.S., R.L., L.S., M.E.J., P.H., and J.L.P. analyzed data; and J.S., A.H., R.R.M., M.S., R.L., P.H., O.S., and J.L.P. wrote the paper.

The authors declare no conflict of interest.

This article is a PNAS Direct Submission.

See Commentary on page 12578.

[1]A.H., R.R.M., M.S., R.L., and L.S. contributed equally to this work.

[2]To whom correspondence should be addressed. Email: jenny_l.persson@med.lu.se.

This article contains supporting information online at www.pnas.org/lookup/suppl/doi:10.1073/pnas.1405801111/-/DCSupplemental.

breast cancer cell line, suggesting that overexpression of PIP5K1α is associated with malignant diseases (31).

In this study we present our discovery of a diketopiperazine fused C-1 indol-3-yl substituted tetrahydroisoquinoline, termed ISA-2011B, as a novel anticancer drug that effectively inhibits growth of PCa tumor in vivo and invasion of PCa cells in vitro. We unravel the role of PIP5K1α as a target for ISA-2011B and as a central factor that regulates PI3K/AKT and AR signaling pathways, which are involved in regulation of cell proliferation, survival, and invasion.

Results

Discovery of ISA-2011B. ISA-2011B, a diketopiperazine fused C-1 indol-3-yl substituted 1,2,3,4-tetrahydroisoquinoline derivative, was discovered as a result of our development of C-1 indol-3-yl substituted 1,2,3,4-tetrahydroisoquinolies via a Pictet-Spengler approach (32) (Fig. 1*A*) and was found to have a potent inhibitory effect on proliferation in various types of aggressive cancer cell lines (Fig. S1). The dose-dependent effect of ISA-2011B on proliferation of PC-3 cells was determined by tetrazolium dye-based proliferation assay (MTS). The proliferation rate of PC-3 cells after treatment with ISA-2011B at 10, 20, and 50 μM was significantly reduced to 58.77%, 48.65%, and 21.62% of vehicle-treated controls, respectively. Mean absorbance for control cells and cells that were treated with 10 μM ISA-2011B were 0.53 and 0.31, respectively [difference, 0.22; 95% confidence interval (CI) 0.26–0.36; $P = 0.003$] (Fig. 1*B*). Further, the effect of ISA-2011B is significantly stronger on PC-3 cells with *PTEN* mutation at 10 μM ($P = 0.0006$) and 50 μM ($P = 0.025$) than on 22Rv1 cells, which contain intact *PTEN* gene (Fig. 1*C*).

One of the most compelling applications of comprehensive high-throughput kinase profiling is the screening of the compound

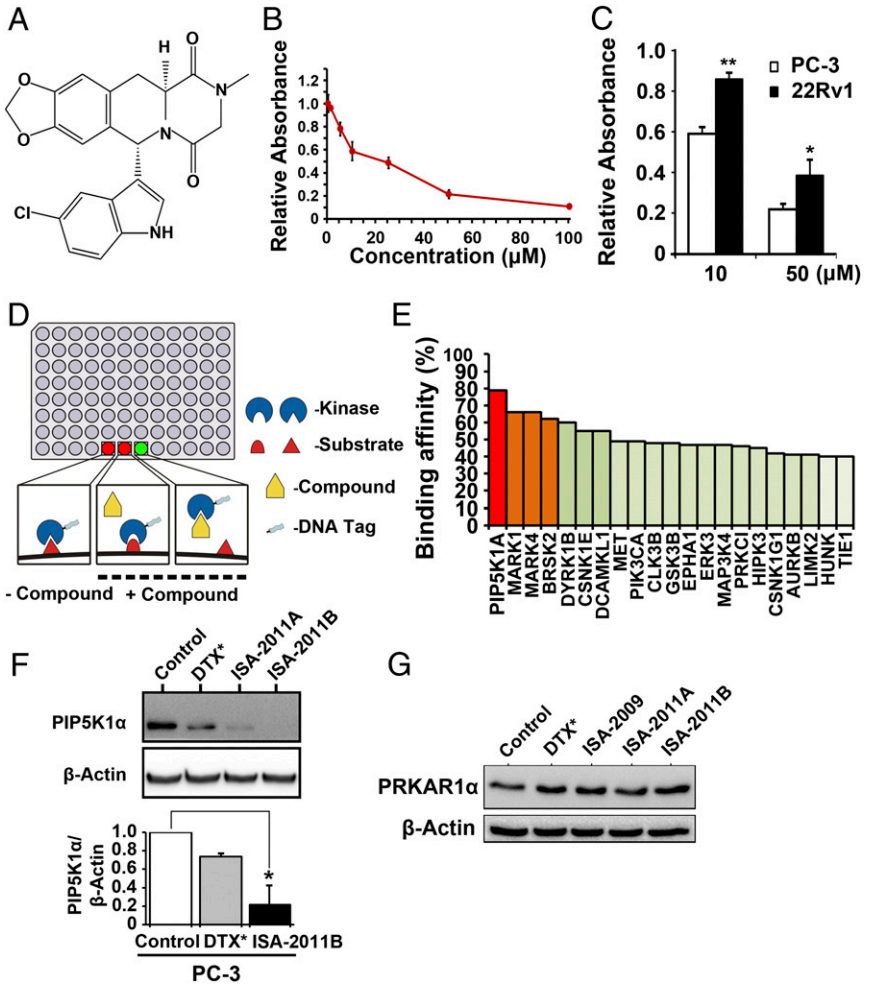

Fig. 1. Characterization of PIP5K1α as a specific target for a novel anticancer compound, ISA-2011B. (*A*) The chemical structure of ISA-2011B. (*B*) Dose-dependent effect of ISA-2011B on proliferation of PC-3 cells was assessed using the nonradioactive MTS proliferation assay. Mean absorbance for control and 10 μM ISA-2011B treated cells were 0.53 and 0.31, respectively (difference = 0.22; 95% CI 0.26–0.36; $P = 0.003$). Mean absorbance for 20 μM ISA-2011B–treated cells was 0.26 (difference = 0.27; 95% CI 0.23–0.29; $P < 0.001$). Mean absorbance for 50 μM ISA-2011B–treated cells was 0.11 (difference = 0.42; 95% CI 0.09–0.14; $P < 0.001$). Data means are from three independent experiments performed with upper 95% CIs. (*C*) Difference in the effect of ISA-2011B on proliferation between PC-3 cells and 22Rv1 cells. The effect of ISA-2011B on PC3 cells at 10 μM ($P = 0.0006$) and 50 μM ($P = 0.025$) is significantly stronger than on 22Rv1 cells. Data means are from three independent experiments. *$P < 0.05$, **$P < 0.01$. (*D*) Schematic illustration on high-throughput kinase profiling technology using the KINOMEscan platform. Bound kinase levels in test compound and control wells are compared. The experiments were performed in triplicate. (*E*) Binding affinity of ISA-2011B with PIP5K1α and a group of kinases, obtained from the assay indicated in *D*. (*F*) PC-3 cells were treated with DMSO as control, docetaxel (DTX) at 50 nM, and ISA-2011B and its analog 2011A at 20 μM for 48 h. Protein lysates from each treatment were subjected to immunoblot analysis. Antibody against PIP5K1α was used as a probe. Data are the means of three independent experiments. *$P < 0.05$. (*G*) PC-3 cells were treated with DMSO as control, docetaxel (DTX) at 50 nM, and ISA-2009, ISA-2011B, and 2011A at 20 μM for 48 h. Antibody against PRKAR1α was used as a probe for immunoblotting.

across a panel of kinases to identify the binding targets (33). We screened ISA-2011B across 460 kinases covering more than 80% of the human catalytic protein kinome (Fig. 1*D*). ISA-2011B exhibited the highest binding affinity to PIP5K1α, and to MAP/microtubule affinity-regulating kinase 1 and 4 (MARK1 and MARK4) as well (Fig. 1*E*). Because PIP5K1α is linked to PI3K/AKT pathways, it was selected for further validation. ISA-2011B treatment inhibited PIP5K1α expression by 78.6% in PC-3 cells, as determined by immunoblot analysis (Fig. 1*F*). As measured by densitometric quantification of the blots from three independent experiments using the ImageJ program, the mean value of PIP5K1α expression was 9.43 in control cells, compared with 2.01 in ISA-2011B–treated cells (95% CI 0.31–4.34; $P = 0.013$) (Fig. 1*F*). ISA-2011A, an analog of ISA-2011B, also reduced the level of PIP5K1α, but treatment with a taxane-based drug (docetaxel) did not markedly inhibit PIP5K1α expression (Fig. 1*F*). However, ISA-2011B did not inhibit cAMP-dependent protein kinase type I-alpha regulatory subunit (PRKAR1α), a key receptor of cAMP/PKA, which also activates AKT (34) (Fig. 1*G*). Collectively these results indicate that ISA-2011B inhibits PIP5K1α but not proteins that are unrelated to PIP5K1α.

ISA-2011 Effectively Inhibited Tumor Growth in Xenograft Mouse Models. The most significant preclinical extension of this work is to determine the therapeutic benefit of ISA-2011B in vivo. We examined the effect of ISA-2011B on growth of invasive human prostate tumor grafted into mice. When the mean tumor volume reached 50 mm^3, treatment of xenograft mice with vehicle control, ISA-2011B, docetaxel, and a combination of ISA-2011B and docetaxel was initiated and lasted for 20 d. Growth of tumors in mice treated with ISA-2011B regressed compared with tumors in control (Fig. 2*A*; mean volume of vehicle control = 500.00 mm^3, ISA-2011B treated = 42.00 mm^3, difference = 458.00 mm^3; 95% CI 7.70–76.30; $P < 0.001$, two-sided *t* test). Similarly, this was also the case for tumors treated with ISA-2011B and docetaxel in a combination (Fig. 2*A*; mean volume of ISA-2011B + docetaxel-treated group = 36.00 mm^3; 95% CI 30.40–41.60; $P < 0.001$, two-sided *t* test). Although tumors treated with docetaxel also regressed (Fig. 2*A*), adverse effects of docetaxel on mice were pronounced. In contrast, no adverse effect such as weight loss was observed in mice treated with ISA-2011B and docetaxel in combination. This suggests that ISA-2011B interacts with docetaxel to reduce its off-target effects with unknown mechanisms. On day 20, tumor mass of the treatment groups was significantly smaller compared with that of the control group (Fig. 2*B*; compared with control, for ISA-2011B treated, $P < 0.006$; for ISA-2011B + docetaxel, $P < 0.001$).

Effect of ISA-2011B on Tumor Growth Is Associated with Its Effect on PIP5K1α, Which Is Highly Expressed in Human PCa. The most important step during drug development is to characterize the associations between target and disease and to explore the potential role of the new targets. Having identified a significant anticancer effect of ISA-2011B in PCa growth in vivo, we went on to study the clinical importance of PIP5K1α in PCa patient samples. A tissue microarray that contained biopsies of benign prostate hyperplasia (BPH) and paired cancer tissues from 48 PCa patients were immunostained with antibodies against PIP5K1α, PIP2, and AR (Fig. 3*A*). PIP5K1α, PIP2, and AR expression were significantly higher in PCa tissues compared with BPH epithelium, as determined by Wilcoxon's signed rank test ($P < 0.001$) (Fig. 3*B*). There was a significantly positive correlation between PIP5K1α and PIP2 ($r^2 = 0.477$, $P = 0.01$) and between PIP5K1α and AR ($r^2 = 0.640$, $P = 0.01$), as determined by Spearman's rank correlation test.

We next examined genes encoding PIP5K1α, AKT1, AKT2, PTEN, and AR in primary ($n = 181$) and metastatic ($n = 37$) PCa tissues by using a public database (35). We observed alterations in genes encoding PIP5K1α, AKT2, PTEN, and AR in subsets of PCa patients (Fig. S2). A Mann–Whitney test revealed that expression of *PIP5K1A*, *AKT2*, and *AR* was significantly higher in metastatic lesions compared with primary PCa ($P < 0.001$)

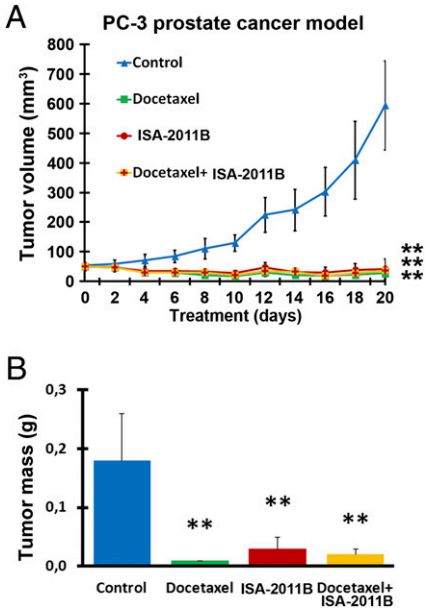

Fig. 2. Effect of ISA-2011B on growth of PC-3 tumor xenografts in vivo. (*A*) Growth of tumor xenografts treated with vehicle (Control), docetaxel (10 mg/kg), ISA-2011B (40 mg/kg), and docetaxel (10 mg/kg) in combination with ISA-2011B (40 mg/kg) every second day. Treatment started on day 0 and ended on day 20 ($n = 6$ mice per group). Mean tumor volumes and upper 95% CIs are shown. $^{**}P < 0.01$. (*B*) Tumors from each group were collected and weighted at the end of experiment. On day 20, mean tumor mass of control group = 0.183 g, ISA-2011B treated group = 0.027 g, difference = 0.156 g; 95% CI = 0.012–0.041; $P < 0.006$; ISA-2011B + docetaxel treated group = 0.024 g, difference = 0.159 g; 95% CI = 0.016–0.031; $P < 0.001$. Mean tumor mass in grams and upper 95% CIs are shown. $^{**}P < 0.01$.

(Fig. 3*C*). Gene amplification in *PIP5K1A* was observed in 2.8% ($n = 5$ of 181) of primary cancer and 16.2% ($n = 6$ of 37) of metastatic PCa lesions ($P = 0.001$). The follow-up time from diagnosis to disease recurrence known as biochemical recurrence (BCR) ranged from 1 to 168 mo (Fig. 3*D*). A subset of patients with higher mRNA expression due to gene amplifications in *PIP5K1A*, *AKT2*, and *AR* or low mRNA expression due to PTEN mutation suffered poorer BCR-free survival (for *PIP5K1A*, $P < 0.001$; for *AKT2*, $P = 0.01$; for *AR*, $P < 0.001$) (Fig. 3*D* and Fig. S3). Thus, overexpression of *PIP5K1A*, *AKT2*, and *AR* or down-regulation of *PTEN* is associated with poor prognosis of PCa patients.

Overexpression of PIP5K1a Increased Expression of Cell Proliferation Markers and Invasiveness. We further characterized the consequence and molecular mechanisms of PIP5K1α overexpression in PCa cells. Expression of PIP5K1α, pSer-473 AKT, and the key cell cycle regulators cyclin D1 and cyclin-dependent kinase 1 (CDK1) was detected in nonmalignant cells at relatively lower levels compared with the malignant PCa cells (Fig. 4*A*). We introduced overexpression of PIP5K1α by transfecting nonmalignant PNT1A cells with pLPS-PIP5K1α-EGFP vector or pLPS-EGFP control. As determined by immunostaining of cells with antibodies against PIP5K1α, β-tubulin, and PIP2, we observed that overexpression of PIP5K1α led to an enhanced β-tubulin and PIP2 expression in PNT1A cells (Fig. 4 *B* and *C*). Overexpression of PIP5K1α led to an increase in PIP5K1α protein expression by 47.61% compared with control ($P = 0.047$) (Fig. 4*D*). This was coincident with the effect of PIP5K1α overexpression on AKT activation. Expression of pSer-473 AKT increased by 666.81% in PNT1A cells transfected with pLPS-PIP5K1α compared with controls (Fig. 4*D*; control transfected mean = 3.78; PIP5K1α transfected mean = 29.02, difference = 25.24; 95% CI 21.67–36.37; $P = 0.021$). Thus, PIP5K1α overexpression significantly increased activity of AKT. It is known that AKT, once activated, will go on to regulate multiple

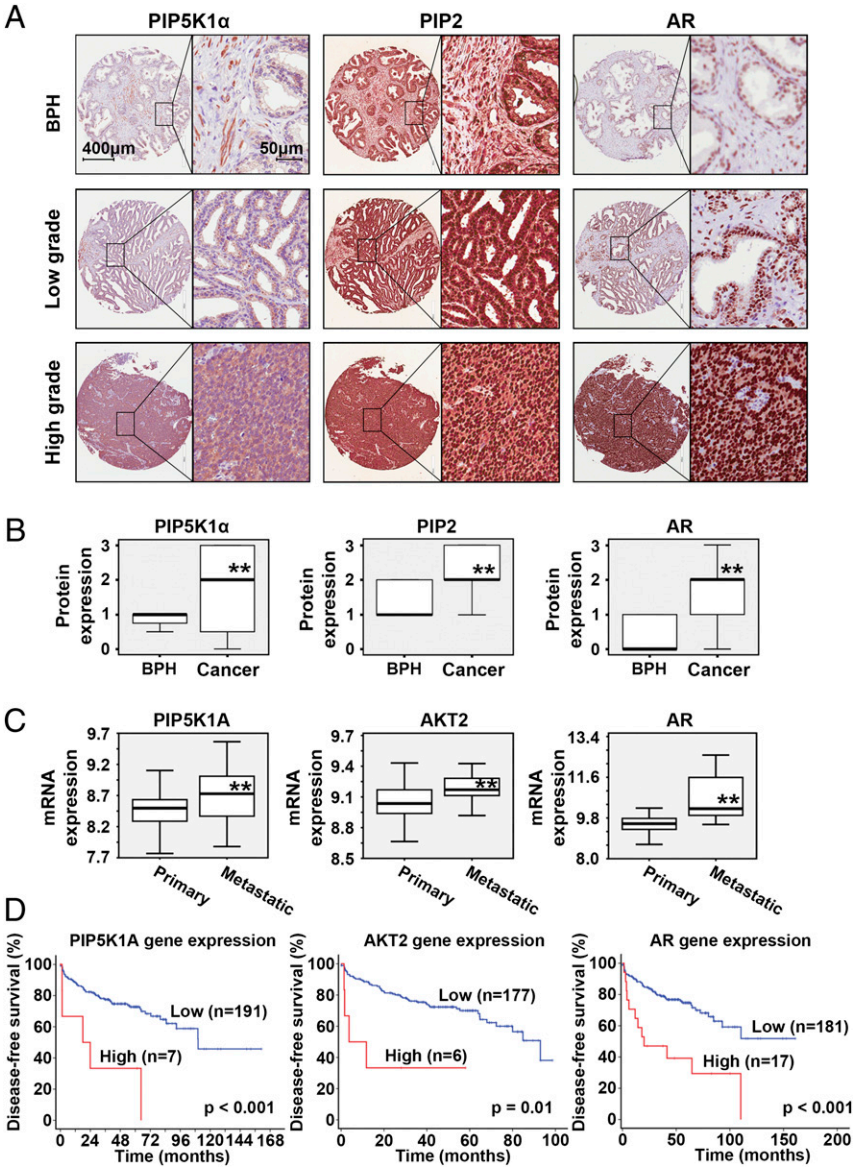

Fig. 3. Evaluation of the clinical importance of PIP5K1α and its link with PIP2 and AR in PCa patients. (*A*) Immunohistochemical analysis of a tissue microarray containing BPH and paired PCa specimens from 48 PCa patients. Representative microphotographs are shown. Scale bars are indicated and are applied to all images in *A*. (*B*) Box-plot quantitative comparison between BPH and paired cancer specimens from 48 PCa patients. The paired Wilcoxon's rank sum test analyses are shown for PIP5K1α, PIP2, and AR. $^{**}P < 0.01$. (*C*) Box plots presenting expression of genes encoding PIP5K1α, AKT2, and AR. Tumor specimens from distinct subgroups of patients with primary ($n = 181$) and metastatic ($n = 37$) PCa were assessed. $^{**}P < 0.01$. (*D*) Kaplan-Meier survival analysis based on BCR-free, showing the difference between patients with low or high expression of the regulators. Differences in BCR-free survivals between two groups were calculated using the log–rank test.

factors that control cell cycle proliferation, survival, invasion, and metastasis via its kinase activity (36). Expression of the G0/G1 and S/G2/M cyclins and CDKs including cyclin D1, cyclin E1, cyclin A2, CDK1, and cyclin B1 was increased in PNT1A cells that overexpressed PIP5K1α compared with controls (Fig. 4 *E* and *F*). PIP5K1α overexpression also resulted in an induction of a series of key factors, downstream or upstream of AKT. These included phosphorylation of focal adhesion kinase (FAK), a focal adhesion molecule; Twist 1, a proinvasion regulator (Fig. 4*G*), and vascular endothelial growth factor (VEGF) and matrix metalloproteinase 9 (MMP9), the factors that mediate angiogenesis (Fig. 4*H*). We further assessed whether PNT1A cells overexpressing PIP5K1α may have gained malignant invasive feature by performing an invasion assay. PNT1A cells overexpressing PIP5K1α gained the ability to invade through the extracellular matrix-coated membrane, with an invasive capacity of 412% higher than in controls ($P = 0.014$) (Fig. 4*I*). Interestingly, overexpression of PIP5K1α greatly increased expression of AR, as determined by immunoblot analysis (Fig. 4*J*) and immunostaining (Fig. S4). Immunoprecipitation assays further revealed that AR formed protein–protein complexes with CDK1 in the nuclear compartment of PNT1A cells expressing control vector or PIP5K1α vector (Fig. 4*K* and Fig. S5). Thus, PIP5K1α is able to activate the PI3K/AKT pathway and enhance cross-interactions of AKT with AR, probably through CDK1.

ISA-2011B Inhibits the Elevated Survival, Proliferation, and Invasion Signaling. As demonstrated in Fig. 3*A*, PIP5K1α is highly expressed in primary and metastatic PCa and in androgen-dependent malignant LNCaP cells. We next tested whether inhibition of PIP5K1α by ISA-2011B might lead to successful inhibition of deregulated

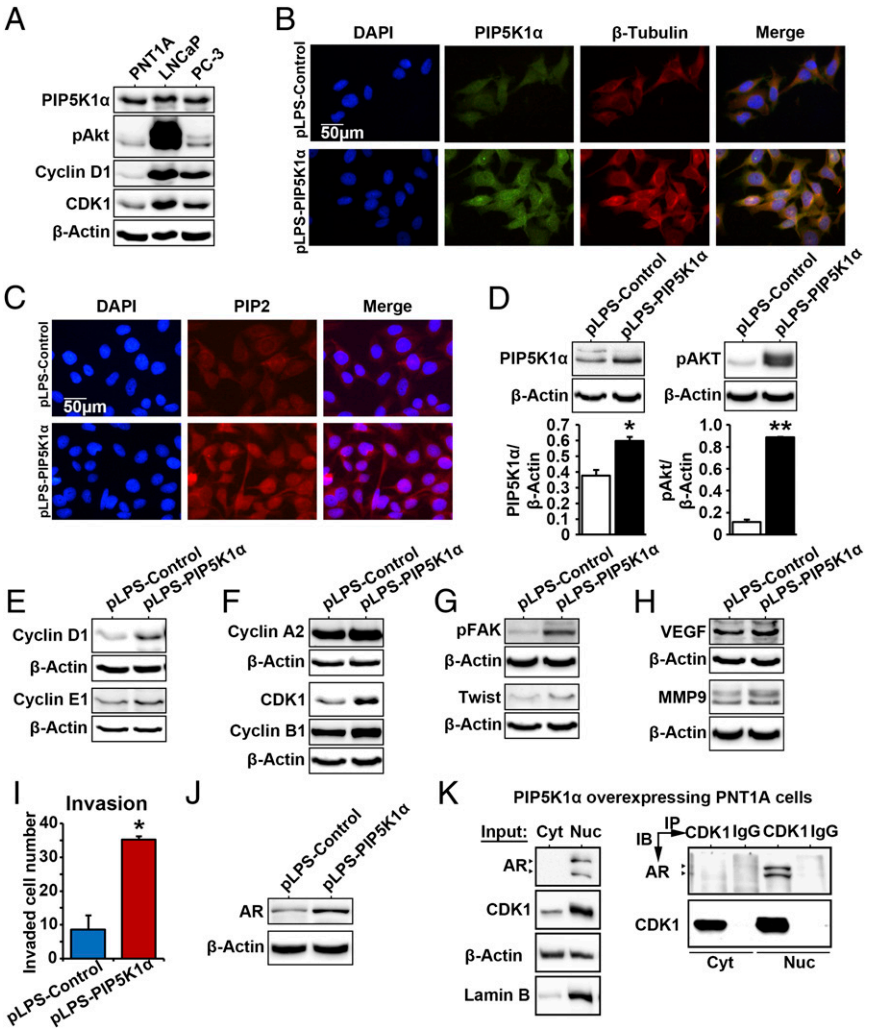

Fig. 4. PIP5K1α overexpression promotes malignant phenotype in nonmalignant epithelial PNT1A cells via AKT/AR/CDK1 pathways. (*A*) Immunoblots show the expression of PIP5K1α, phosphorylated AKT, cyclin D1, and CDK1 in a panel of PCa cell lines including PNT1A, LNCaP, and PC-3. (*B*) Effect of PIP5K1α overexpression on the morphology of PNT1A cells. Representative immune-fluorescent images show the overexpression of PIP5K1α and its colocalization with β-tubulin. DAPI was used to stain the nucleus of cells. The scale bar is indicated. (*C*) Representative images of the immunofluorescent cells overexpressing PIP5K1α or control vector, stained with PIP2 antibody. (*D*) Immunoblots show the effect of PIP5K1α overexpression on PNT1A cells. The mean expression of PIP5K1α in cells transfected with pLPS-EGFP control vector was 7.42, and the mean value in cells transfected with pLPS-PIP5K1α was 10.96 (difference = 3.54; 95% CI 5.89–16.02; $P = 0.047$). The mean expression of AKT in cell transfected with pLPS-EGFP control vector was 3.78, and the mean value in cells transfected with pLPS-PIP5K1α was 29.02 (difference = 25.24; 95% CI 21.67–36.37; $P = 0.021$). Data are presented as the average of three independent experiments (±SD). $^*P < 0.05$. $^{**}P < 0.01$. (*E*) Immunoblots show the effect of overexpression of PIP5K1α on cyclin D1, cyclin E1, and (*F*) cyclin A2, CDK1, and cyclin B1 or (*G* and *H*) phosphorylated FAK, Twist, VEGF, and MMP9 in PNT1A cells. (*I*) The number of invaded cells is indicated. Data are presented as an average of triplicates (±SD). $^*P = 0.014$. (*J*) Immunoblots show the expression of AR in PNT1A cells overexpressing PIP5K1α or control vector. (*K*) Cytoplasmic (Cyt) and nuclear (Nuc) fractions were separated from PNT1A cells overexpressing PIP5K1α. Cells were subjected to immunoprecipitation (IP) assay as shown (*Right*). Antibody to CDK1 was used to pull down the immunocomplexes, and antibody to IgG was used as a negative control. Antibodies against AR or CDK1 were used for immunoblot analysis (IB). The cell lysates from cytoplasmic and nuclear fractions were used as "Input" controls as indicated (*Left*). Blotting of actin served as loading control, and antibody against lamin B was used as a control for the nuclear fraction.

PI3K/AKT and AR pathways. Treatment of LNCaP cells with ISA-2011B and its analog ISA-2011A reduced PIP5K1α expression (Fig. 5*A*) and inhibited proliferation of LNCaP cells (Fig. S6). ISA-2011B significantly inhibited pSer-473 AKT, by 75.55% compared with control (Fig. 5*B*; mean pSer-473 AKT expression in control treated = 13.43, mean expression in ISA-2011B treated = 10.15, difference = 3.28; 95% CI = 3.34–16.95; $P = 0.026$). However, expression of pSer-473 AKT was not affected by etoposide, docetaxel, and tadalafil, an approved drug for treatment of BPH, which exhibits slight similarity in the chemical structure compared with ISA-2011B (Fig. 5*B*). The expression of pSer-473 AKT was barely detectable in ISA-2011B–treated cells, which displayed characteristics of apoptotic bodies and fragmented nucleus (Fig. 5*C*). In contrast, expression of phosphorylated cAMP response element-binding protein (CREB), a downstream factor of the PKA pathway, remained unchanged in cells treated with ISA-2011B, ISA-2011A, etoposide, tadalafil, and docetaxel (Fig. 5*D*). ISA-2011B treatment led to a down-regulation of CDK1 (Fig. 5*E*). Interestingly, ISA-2011B treatment inhibited SKP2, a key ubiquitin enzyme that mediates P27 degradation, and ISA-2011B increased expression of P27, an inhibitor that is required to block cell proliferation by inhibiting cyclins and CDKs (Fig. 5*F*). ISA-2011B treatment also led to a remarkable inhibition of AR and prostate-specific antigen (PSA) expression (Fig. 5 *G* and *H*). However, docetaxel, ISA-2009, and ISA-2011A had no effect on

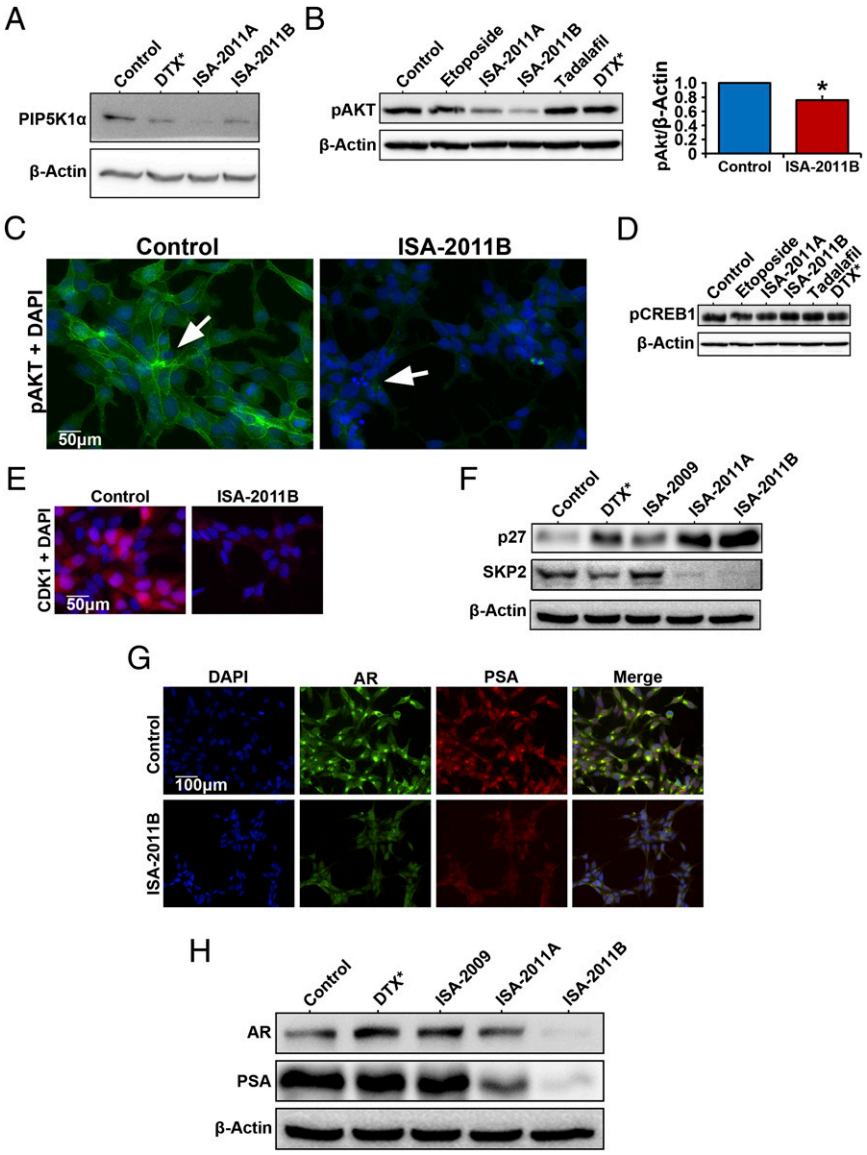

Fig. 5. Effect of ISA-2011B on PIP5K1α and its downstream regulators in androgen-sensitive LNCaP cells. (*A*) LNCaP cells were treated with docetaxel at 50 nM and ISA-2011B (20 μM), and the lysates were subjected to immunoblot analysis. Antibodies against PIP5K1α and β-actin were used. (*B*) LNCaP cells were treated with DMSO as vehicle control (Control), etoposide (20 μM), ISA-2011A (20 μM), ISA-2011B (20 μM), tadalafil (20 μM), and docetaxel (DTX) at 50 nM. Quantification of the immunoblots of phosphorylated AKT in LNCaP cells treated with vehicle control or ISA-2011B are shown. Data are representative of three independent experiments. $*P < 0.05$. (*C*) Representative immunofluorescent images show the expression and subcellular localization of phosphorylated AKT in LCaP cells treated with vehicle control or ISA-2011B. (*D*) Immunoblots show the expression of phosphorylated CREB in LCaP cells treated with different agents as indicated. (*E*) Representative immunofluorescent images show the expression and subcellular localization of CDK1 in LCaP cells treated with vehicle control or ISA-2011B. (*F*). LNCaP cells were treated with docetaxel (50 nM), ISA-2009, ISA-2011A, and ISA-2011B (20 μM). The lysates were subjected to immunoblot analysis using antibodies against P27 and SKP2 as probes. (*G*) Representative immunofluorescent images show the expression and subcellular localization of AR and PSA in LNCaP cells treated with vehicle control or ISA-2011B. (*H*) Immunoblots show the expression of AR and PSA in LNCaP cells that were treated with docetaxel (50 nM), ISA-2009, ISA-2011A, and ISA-2011B (20 μM).

AR and PSA expression (Fig. 5*H*). These data suggest that the ISA-2011B–mediated inhibitory effect on PCa proliferation is associated with its ability to inhibit PIP5K1α, which transduces the inhibitory effect to its downstream signaling pathways, including AKT, AR, and cell cycle.

ISA-2011B Targets PIP5K1α/AKT/AR Pathways to Inhibit Tumor Cell Growth and Induce Apoptosis in Aggressive PCa Cells. We further tested whether inhibition of PIP5K1α by ISA-2011B might lead to successful inhibition in cancer cell invasion in PC-3 cells. A live cell imaging system, Holomonitor M3 imaging analysis, was used to monitor the effect of ISA-2011B, etoposide, and docetaxel on morphological changes in living cells in real-time for up to 48 h. ISA-2011B treatment led to a reduction in cell size and changes in morphology, which was also achieved by docetaxel treatment (Fig. 6*A*). PI3K activates AKT signaling pathways through PIP2 and PIP3 (17). PIP3 expression was greatly reduced in viable cells and was barely detectable in cells with fragmented nucleus after ISA-2011B treatment (Fig. 6*B*). Similar to what was observed in LNCaP cells that were treated with ISA-2011B, the decreased PIP5K1α was coincident with a reduced expression of phosphorylated AKT in PC-3 cells treated with ISA-2011B. The mean pSer-473 AKT expression in control treated cells was 18.44, compared with 5.49 in ISA-2011B–treated

cells, with a decrease down to 29.77% (difference = 12.95; 95% CI = 2.84–8.14; $P = 0.001$) (Fig. 6*C*). Similar to what was observed in LNCaP cells, etoposide, tadalafil, and docetaxel did not exhibit an inhibitory effect on AKT activity in PC-3 cells (Fig. 6*C*). Expression of the key cell cycle regulators, including cyclin D1, cyclin E1, cyclin A2, CDK1, phosphorylated CDK1, and cyclin B1, was remarkably inhibited by ISA-2011B (Fig. 6 *D* and *E*). ISA-2011B treatment led to an accumulation of cells at G2/M phase of the cell cycle, a characteristics of cells that are unable to undergo proliferation (mean G2/M phase cells in control group is 14.87% and in treated group is 19.83%; difference = 4.96%; 95% CI 15.01–20.79%; $P = 0.047$) (Fig. 6*F*). In contrast to docetaxel, ISA-2011B treatment led to an increased rate of apoptosis, with a constant rate of unspecific necrosis in PC-3 cells compared with controls ($P < 0.001$) (Fig. 6*G*). Because the cell–cell attachment is essential for cancer cells to expand and invade, we tested whether ISA-2011B may prevent adherence and attachment of PC-3 cells. PC-3 cells treated with ISA-2011B or solvent were subjected to adhesion assay (Fig. 6*H*). The

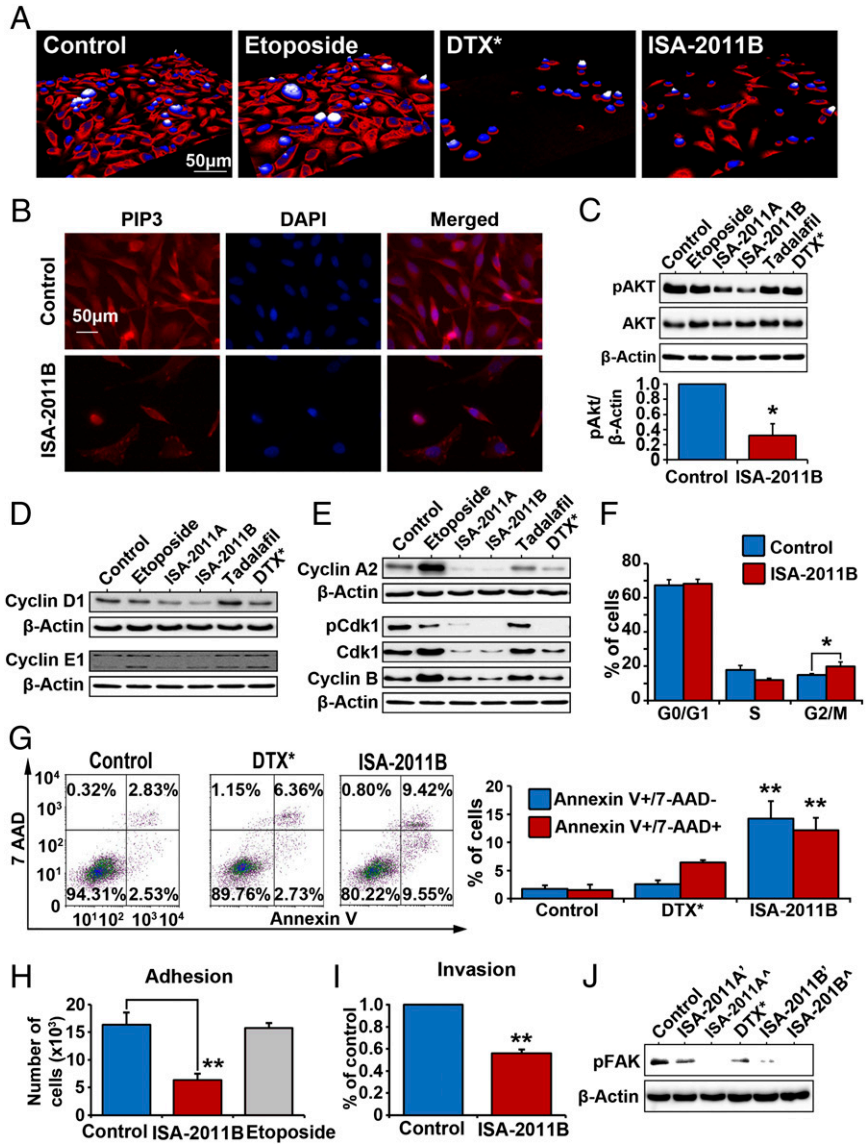

Fig. 6. ISA-2011 inhibits tumor invasion through inhibition PIP5K1α-mediated cancer cell pathways. The Holomonitor M3 imaging system was applied to capture living PC-3 cells in culture during treatment. (*A*) Representative microphotographs of PC-3 cells treated with vehicle control, etoposide (50 μM), docetaxel (100 nM), and ISA-2011B (50 μM) for 48 h. The scale bar is indicated. (*B*). Representative immunofluorescent images show the expression and subcellular localization of PIP3 in PC-3 cells treated with vehicle control or ISA-2011B. The scale bar is indicated. (*C*) PC-3 cells were treated with vehicle control (DMSO), 50 μM of etoposide, ISA-2011A, ISA-2011B, tadalafil, and docetaxel (DTX) at 100 nM for 48 h. The protein lysates were subjected to immunoblots. Antibodies to phosphorylated AKT and total AKT were used as probes. Data are representative of three independent experiments. *$P < 0.05$. (*D* and *E*) Immunoblots shows the expression of the key cell cycle proteins in PC-3 cells treated with different agents as indicated. (*F*) Cell cycle distribution of PC-3 cells treated with vehicle control or ISA-2011B. (*G*) Representative FACS plots show the apoptosis status of cells treated with DMSO as vehicle control, docetaxel (DTX), or ISA-2011 (*Left*). Data are representative of three independent experiments. **$P < 0.01$ (*Right*). (*H*). Adhesion assay of PC-3 cells treated with DMSO as vehicle control, etoposide, and ISA-2011B. Plates were coated with fibronectin before seeding the cells. Mean number of adherent cells in control is 1.62×10^4; mean adherent cells treated with ISA-2011B is 0.63×10^4 (difference = 0.99×10^4; 95% CI 0.53×10^4 to 0.77×10^4; $P = 0.002$). Data are representative of three independent experiments. Upper 95% confidence intervals are shown. **$P < 0.01$ (*Right*). (*I*) Invasion assays of PC-3 cells treated with DMSO as vehicle control or ISA-2011B. (*J*) Immunoblots of phosphorylated FAK in PC-3 cells after 48 h treatment with DMSO as vehicle control, docetaxel (DTX) at 500 nM, and ISA-2011A and ISA-2011B ('20 μM and ^50 μM).

rate of adherence in cells treated with ISA-2011B was only 38.82% compared with that of control ($P = 0.002$) (Fig. 6*H*). We further assessed the effect of ISA-2011B on invasiveness of PC-3 cells using an invasion assay. ISA-2011B inhibited invasiveness of PC-3 cells down to 55.96% of control (Fig. 6*I*). Mean absorbance in control was 0.121; mean absorbance in ISA-2011B treated cells was 0.068 (Fig. 6*I*; difference = 0.053; 95% CI 0.066–0.070; $P < 0.001$). Expression of phosphorylated FAK, a factor that promotes invasion, was almost diminished in PC-3 cells treated with ISA-2011B and ISA-2011A in a dose-dependent fashion (Fig. 6*J*). However, docetaxel did not show a pronounced effect on FAK phosphorylation (Fig. 6*J*). Taken together, ISA-2011B inhibits proliferation, survival, and invasion in androgen-insensitive PCa cells. Moreover, this effect may be mediated through PIP5K1α and its downstream PI3K/AKT.

The Effect of Depletion of PIP5K1α in PC-3 Cells. We next asked whether inhibition of PIP5K1α via siRNA-mediated knockdown may achieve the same effect as that of ISA-2011B treatment in PC-3 cells. As such, we silenced PIP5K1α by transfecting PC-3 cells with PIP5K1α or scramble siRNA. Immunoblot analysis confirmed that expression of PIP5K1α was reduced to 34.45% in cells transfected with PIP5K1α siRNA compared with control. Mean PIP5K1α expression in control was 13.49; mean value in PIP5K1α knockdown was 4.65 (Fig. 7*A*; difference = 8.84; 95% CI = 3.86–5.43; $P < 0.001$). Knockdown of PIP5K1α resulted in a significant decrease in expression of pSer-473 AKT, down to 57.88%. Mean pSer-473 AKT in control was 29.46 and was 17.05 in PIP5K1α knockdown cells (Fig. 7*B*; difference = 12.41; 95% CI 7.80–26.31; $P = 0.007$). Thus, the effect of inhibition of PIP5K1α via siRNA on AKT activation was equivalent to what was achieved by ISA-2011B treatment. The expression of cyclin D1, cyclin A2, CDK1, and cyclin B1 was decreased in PC-3 cells transfected with PIP5K1α siRNA compared with controls (Fig. 7 *C* and *D*). The morphology of PC-3 cells expressing siPIP5K1α, as determined by β-tubulin staining, exhibited remarkable differences compared with PC-3 cells expressing control siRNA but was similar to control PNT1A cells (Fig. 7*E*). Conversely, the morphology of PNT1A cells overexpressing PIP5K1α resembled aggressive PC-3 control cells (Fig. 7*E*). The activation of FAK was reported to be linked to a switch toward aggressive phenotypes. Expression of phosphorylated FAK in PC-3 cells expressing siPIP5K1α decreased to 36.98% ($P < 0.001$). Depletion of PIP5K1α led to an increase in P27 expression and a decrease in twist 1 and MMP9 (Fig. 7*G*). An apoptotic marker, cleaved poly (ADP-ribose) polymerase (c-PARP), is used to detect early apoptotic process. Immunoblot analysis for c-PARP expression was performed using lysates from PC-3 cells transfected with control siRNA or siPIP5K1α, which were treated with ISA-2011B or vehicle (Fig. 7*H*). Two distinct isoforms of c-PARP were detected in PC-3 cells that were either treated with ISA-2011B at 50 μM alone, expressed siPIP5K1α alone, or expressed siPIP5K1α

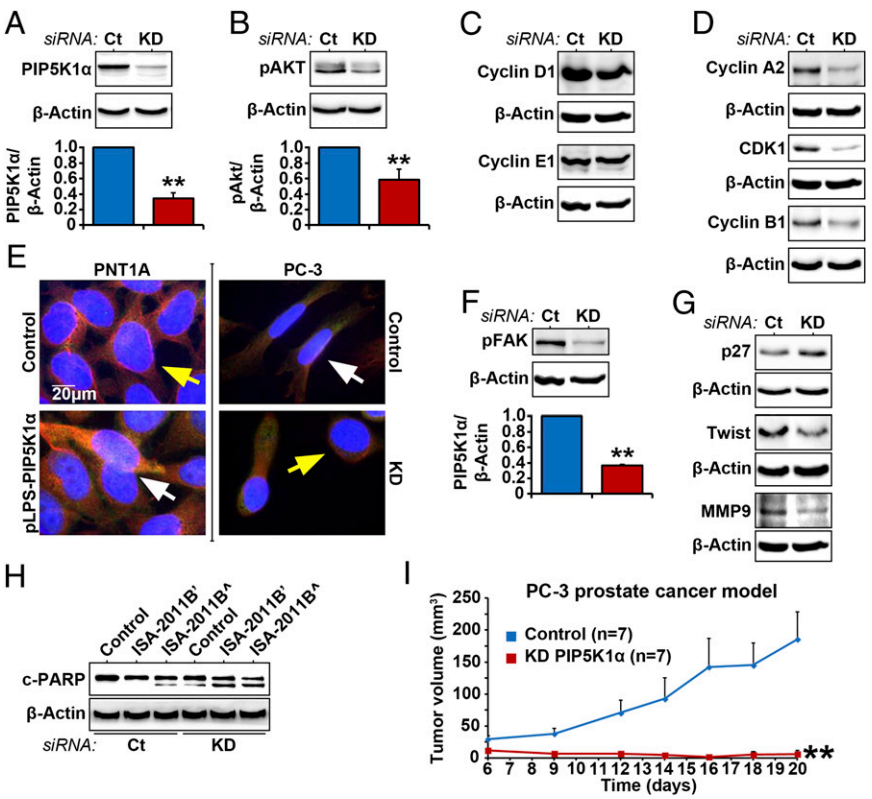

Fig. 7. Effect of PIP5K1α inhibition on AKT pathways in PC-3 cells. (*A* and *B*) PIP5K1α was depleted by transfecting PC-3 cells with PIP5K1α siRNA (KD) or scramble control (Ct). Immunoblots for PIP5K1α and phosphorylated AKT in PC-3 cells that were transfected with PIP5K1α siRNA (KD) or scramble control (Ct) are shown. Data are presented as average of three independent experiments (±SD). $^{**}P < 0.01$. (*C* and *D*) Immunoblots showing the effect of PIP5K1α knockdown on cyclin D1, cyclin A2, CDK1, and cyclin B1 in PC-3 cells. (*E*) Morphology of PC-3 cells expressing siRNA to PIP5K1α and PNT1A cells overexpressing PIP5K1α. Antibody to α-tubulin was used for staining. The scale bar is indicated. (*F*) Immunoblots of phosphorylated FAK in PC-3 cells transfected with PIP5K1α siRNA or scramble control. Data are presented as average of three independent experiments (±SD). Mean expression of phosphorylated FAK in control was 15.30, and in PIP5K1α knockdown was 5.66 (difference = 9.58; 95% CI 4.89–6.42; $P < 0.001$). (*G*) Immunoblots of P27, Twist, and MMP9 in PC-3 cells transfected with PIP5K1α siRNA or scramble control. (*H*) Immunoblots of c-PARP in PC-3 cells treated with vehicle control (DMSO) or ISA-2011B ('20 μM and ^50 μM), with or without PIP5K1α or scramble siRNA cotransfection. (*I*) s.c. xenografts were established by implanting PC-3 cells expressing control scramble siRNA or PIP5K1α-siRNA into nude mice. The tumors were measured on day 6 after implantation and were followed for a total of 20 d ($n = 7$ mice per group). Two groups of mice bearing PC3 cells that expressed control siRNA (Control) or PIP5K1α-siRNA (KD-PIP5K1α) are indicated. Difference in tumor growth between the two groups is calculated. $^{**}P = 0.008$.

and were treated with ISA-2011B in combination. This suggests that down-regulation of PIP5K1α through treatment or knockdown induced apoptosis (Fig. 7*H*). We examined the effect of inhibition of PIP5K1α on tumor growth by implanting PC-3 cells expressing control siRNA or siPIP5K1α into nude mice. PC-3 cells expressing control siRNA formed tumors, with the mean tumor volume of 148.5 mm^3 on day 20. In contrast, PC-3 cells transfected with siPIP5K1α barely gave rise to tumors, with a mean tumor volume of 4.9 mm^3 on day 20 [Fig. 7*I*; mean volume of control siRNA tumors = 148.5 mm^3; mean volume of siPIP5K1α = 4.9 mm^3 (only one mouse had tumor); difference = 143.6 mm^3; 95% CI = −4.7, 14.4; $P = 0.008$, two-sided t test]. Taken together, the targeted inhibition of PIP5K1α and ISA-2011B treatment showed similar inhibitory effects on tumor growth in xenograft mice.

Discussion

In this study, we present our discovery of a drug candidate, ISA-2011B, and the role of PIP5K1α, a target of ISA-2011B in PCa progression. ISA-2011B has a unique structure consisting of a diketopiperazine fused, methylenedioxy protected, 1,2,3,4-tetrahydroisoquinoline core with an electron-rich transsubstituent at position 1. We show that ISA-2011B inhibits tumor growth by inhibiting the expression and activity of PIP5K1α, thereby affecting the downstream PI3K/AKT, AR, and cell cycle pathways (Fig. 8). We show, to our knowledge for the first time, that overexpression of PIP5K1α in nonmalignant PNT1A cells induces the invasive capacity of these cells and increases expression of VEGF, phosphorylated FAK, Twist, and MMP9, the key factors that promote cancer cell proliferation and invasion. Conversely, inhibition of PIP5K1α in PC-3 cells via siRNA-mediated knockdown or ISA-2011B treatment reduces invasiveness, induces apoptosis, and inhibits tumor growth in xenograft mice. PIP5K1α and its associated PIP2 and PIP3 are important lipids for membrane structure and actin polymerization, thus elevated levels of these lipids may lead to malignant transformation and progression of cancer cells into a more invasive phenotype. Our present study suggests that PIP5K1α has a great potential to be used as a drug target for treatment of PCa.

AKT can be activated by phosphorylation through two upstream pathways: through PI3K/PIP3 or through cAMP/PKA (36). In the present study we show that ISA-2011B inhibits AKT activity through PIP5K1α/PI3K/PIP3. In contrast, ISA-2011B treatment has no effect on PKA receptor and the key protein phosphorylated CREB in cAMP/PKA pathway in LNCaP or PC-3 cells. Further, the effect of ISA-2011B is significantly stronger on PC-3 cells with PTEN mutation than on 22Rv1 cells, which contain intact PTEN gene. 22Rv1 cells, although less sensitive to ISA-2011B, also displayed reduced proliferation after ISA-2011B treatment. It is known that 22Rv1 cells also have relatively high levels of pAKT and AR (37). Given that amplification of AKT2 or mutations in PIK3CA, in addition to PTEN mutation, are all responsible for activation of PI3K pathway (15, 38, 39), our data suggest that ISA-2011B exerts its on-target effect on PCa cells by targeting pathways related to AKT/AR, rather than a toxic effect.

The mechanism underlying the interactions between AR and PI3K/AKT still remains poorly understood. In the present study we uncover several unrecognized interlinks among PIP5K1α, PI3K/AKT, AR, and CDK1 in PCa. Previous studies show that the PI3K/AKT and AR pathways negatively regulate each other during castration resistance (38, 39). Our proposed model suggests that ISA-2011B inhibits PIP5K1α, which leads to a subsequent inhibition in PI3K/AKT levels and sustained P27 and down-regulation of CDK1 and other cell cycle regulators. Down-regulation of CDK1 may lead to an inhibition in AR signaling pathways. This model is supported by our data that CDK1 and AR form protein–protein complexes predominantly in the nuclear compartment of cells. The complexes of CDK1–AR are persistent in PNT1A cells overexpressing PIP5K1α. In agreement with our findings, a previously reported study showed that CDK1 phosphorylates AR and thereby activates AR activity during progression of castration-resistant PCa (40). This indicates that ISA-2011B targets CDK1-associated pathways that regulate AR activity.

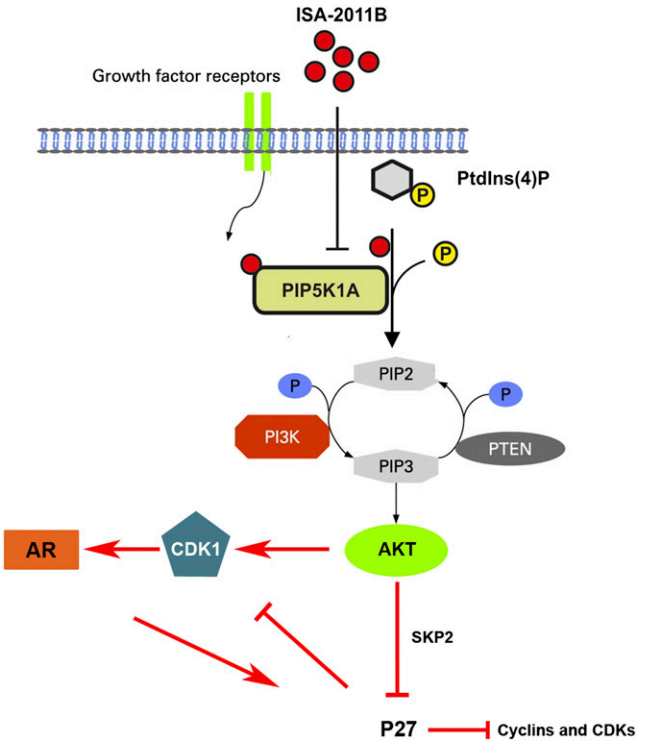

Fig. 8. Schematic model shows the downstream signaling pathway of PIP5K1α and the effect of ISA-2011B inhibition. The model depicts PIP5K1α as the key kinase responsible for generation of PIP2. In turn, PIP2 serves as a precursor molecule required for PI3K activity and generation of PIP3. PIP3 is involved in the downstream activation of AKT, and AKT-related signaling pathways. ISA-2011B is able to enter into the cell and inhibit PIP5K1α. This leads to the reduced production of PIP2 and PIP3 and a subsequent inhibition of PI3K/AKT, but sustained P27 and down-regulation of CDK1 and other cell cycle regulators. Inhibition of AR signaling pathways is mediated through CDK1 in part via a feedback loop.

One of the most significant preclinical extensions of this work is to determine the therapeutic benefit of ISA-2011B in PCa growth. Treatment of xenograft mice with ISA-2011B results in tumor regression. Similarly, PC-3 cells in which PIP5K1α is inhibited through knockdown only formed a small tumor in one out of seven mice, in contrast to control PC-3 cells, which formed large tumors in all seven xenograft mice. These in vivo data are in agreement with the data obtained in cell line studies in which ISA-2011B treatment inhibits tumor growth by inhibiting levels of PIP5K1α and pAKT S473. However, because of the small size of tumors at the end of the experiment, it is difficult to measure the levels of pAKT S473 in vivo.

In the present study we also observed that treatment with ISA2011B in combination with docetaxel completely blocked the progression of invasive PCa locally and profoundly inhibited tumor growth. Docetaxel inhibits mitosis and induces apoptosis in cancer cells as well as normal proliferating cells and is highly toxic. We found that ISA-2011B together with docetaxel showed less toxic effects in mice compared with docetaxel alone. Because the interaction between two drugs often results in changes in metabolic pathways and binding of drugs to cellular membranes, our data suggest that the interaction between ISA-2011B and docetaxel via unknown mechanisms may lead to reduced off-target effects in mice bearing tumors.

Taken together, our findings in the present study provide valuable information on novel targets and anticancer drugs, which hold a great potential for further development of advanced PCa treatment. It will be interesting to further systematically investigate the on-target effect of ISA-2011B treatment on pAKT S473 in vivo by using several well-designed in vivo mouse models in our future studies.

Materials and Methods

KINOMEscan. The interaction of ISA-2011B with 442 kinases covering more than 80% of the human catalytic protein kinome was tested using KINOMEscan assay. Screening "hits" are identified by measuring the amount of kinase captured in test vs. control samples by using quantitative RT-PCR.

Tissue Specimens, Tissue Microarrays, cDNA Microarrays, and CGH Arrays. Tissue microarrays containing BPH and PCa tissues from 48 patients were purchased from Pantomics Inc. mRNA expression data of PIP5K1α, AKT2, PTEN, and AR were extracted from the dataset in the cBioPortal database (35). The study was approved by the Ethics Committee, Lund University, and the Helsinki Declaration of Human Rights was strictly observed.

MTS Proliferation Assay. The effects of ISA-2011B, docetaxel, etoposide, and tadalafil on PCa cell lines and various types of cancer cell lines were determined using the nonradioactive MTS proliferation assay (Promega Biotech) according to the manufacturer's protocol. Viability was determined by measuring the absorbance at 490-nm wavelength, on an Infinite M200 multimode microplate reader (Tecan Sunrise).

Mouse Models of Human Xenograft Tumors. Four sets of treatment experiments in mouse models bearing human PC-3 tumors were performed. All animal experiments met the requirements of the Lund University Animal Care Regulation. For treatment experiments, BALB/c nude mice aged 8 to 12 wk were used in the experiments. Tumor cells (4×10^6) were implanted into the mice (six mice per group). Tumor xenografts were treated with vehicle (control), docetaxel (10 mg/kg), ISA-2011B (40 mg/kg), and docetaxel (10 mg/kg) in combination with ISA-2011B (40 mg/kg) every second day. For PIP5K1α knockdown experiments, 2×10^6 PC-3 cells transfected with control or PIP5K1α siRNA were implanted into the NRMI nude mice (seven mice per group).

Plasmids, Stable Transfection, and siRNA Knockdown Assay. For transfection, pLPS-3′EGFP vector containing full-length human PIP5K1α cDNA as "PIP5K1 α-EGFP" or control empty vector were used. Cells overexpressing PIP5K1α- pLPS-3′EGFP or pLPS-3′EGFP vector were selected by culturing cells in medium containing G418 antibiotics (400 μg/mL) (Sigma–Aldrich).

FACS-Based Cell Cycle Analysis and Apoptosis Assay. Cell cycle analysis of PCa cells after treatment with ISA-2011B was performed. To measure apoptosis, cells were collected after treatment for 48 h and were subsequently stained with FITC-conjugated Annexin V and 7-AAD according to the manufacturer's protocol (BD Biosciences).

Invasion Assay. Boyden transwell chambers were used for the invasion assay according to the manufacturer's protocol (Merck KGaA).

Statistical Analysis. All outcome variables presented are representative of at least three independent experiments. All statistical testes were two-sided, and P values <0.05 were considered to be statistically significant. The statistical software SPSS, version 21 was used.

ACKNOWLEDGMENTS. This work was supported by the grants from the Swedish Cancer Society, The Swedish National Research Council, The Swedish Children Foundation, Malmö Hospital Cancer Foundation, Malmö Hospital Foundation, the Gunnar Nilsson Cancer Foundation, and the Crafoord Foundation (to J.L.P.).

1. Sharma SV, Haber DA, Settleman J (2010) Cell line-based platforms to evaluate the therapeutic efficacy of candidate anticancer agents. *Nat Rev Cancer* 10(4):241–253.
2. Hijikata-Okunomiya A, Okamoto S, Wanaka K (1990) Effect of a synthetic thrombin-inhibitor MD805 on the reaction between thrombin and plasma antithrombin-III. *Thromb Res* 59(6):967–977.
3. Ramnauth J, et al. (2012) 1,2,3,4-tetrahydroquinoline-based selective human neuronal nitric oxide synthase (nNOS) inhibitors: Lead optimization studies resulting in the identification of N-(1-(2-(methylamino)ethyl)-1,2,3,4-tetrahydroquinolin-6-yl)thiophene-2-carboximidamide as a preclinical development candidate. *J Med Chem* 55(6):2882–2893.
4. Oku N, Matsunaga S, van Soest RW, Fusetani N (2003) Renieramycin J, a highly cytotoxic tetrahydroisoquinoline alkaloid, from a marine sponge *Neopetrosia* sp. *J Nat Prod* 66(8):1136–1139.
5. Ferris JP, Guillemin JC (1990) Photochemical cycloaddition reactions of cyanoacetylene and dicyanoacetylene. *J Org Chem* 55(21):5601–5606.
6. Hawkins JM, et al. (1990) Organic chemistry of C60 (Buckminsterfullerene): Chromatography and osmylation. *J Org Chem* 55(26):6250–6252.
7. Brown JR, Auger KR (2011) Phylogenomics of phosphoinositide lipid kinases: Perspectives on the evolution of second messenger signaling and drug discovery. *BMC Evol Biol* 11:4.
8. Engelman JA (2009) Targeting PI3K signalling in cancer: Opportunities, challenges and limitations. *Nat Rev Cancer* 9(8):550–562.
9. Loijens JC, Boronenkov IV, Parker GJ, Anderson RA (1996) The phosphatidylinositol 4-phosphate 5-kinase family. *Adv Enzyme Regul* 36:115–140.
10. Emerling BM, et al. (2013) Depletion of a putatively druggable class of phosphatidylinositol kinases inhibits growth of p53-null tumors. *Cell* 155(4):844–857.
11. Ishihara H, et al. (1996) Cloning of cDNAs encoding two isoforms of 68-kDa type I phosphatidylinositol-4-phosphate 5-kinase. *J Biol Chem* 271(39):23611–23614.
12. Ishihara H, et al. (1998) Type I phosphatidylinositol-4-phosphate 5-kinases. Cloning of the third isoform and deletion/substitution analysis of members of this novel lipid kinase family. *J Biol Chem* 273(15):8741–8748.
13. Loijens JC, Anderson RA (1996) Type I phosphatidylinositol-4-phosphate 5-kinases are distinct members of this novel lipid kinase family. *J Biol Chem* 271(51):32937–32943.
14. Xie Y, Zhu L, Zhao G (2000) Assignment of type I phosphatidylinositol-4-phosphate 5-kinase (PIP5K1A) to human chromosome bands 1q22—> q24 by in situ hybridization. *Cytogenet Cell Genet* 88(3-4):197–199.
15. Shaw RJ, Cantley LC (2006) Ras, PI(3)K and mTOR signalling controls tumour cell growth. *Nature* 441(7092):424–430.
16. Hennessy BT, Smith DL, Ram PT, Lu Y, Mills GB (2005) Exploiting the PI3K/AKT pathway for cancer drug discovery. *Nat Rev Drug Discov* 4(12):988–1004.
17. Saito K, et al. (2003) BTK regulates PtdIns-4,5-P2 synthesis: Importance for calcium signaling and PI3K activity. *Immunity* 19(5):669–678.
18. Somanath PR, Razorenova OV, Chen J, Byzova TV (2006) Akt1 in endothelial cell and angiogenesis. *Cell Cycle* 5(5):512–518.
19. Chen YL, Law PY, Loh HH (2005) Inhibition of PI3K/Akt signaling: An emerging paradigm for targeted cancer therapy. *Curr Med Chem Anticancer Agents* 5(6):575–589.
20. Wang Y, Kreisberg JI, Ghosh PM (2007) Cross-talk between the androgen receptor and the phosphatidylinositol 3-kinase/Akt pathway in prostate cancer. *Curr Cancer Drug Targets* 7(6):591–604.
21. Culig Z, et al. (1999) Switch from antagonist to agonist of the androgen receptor bicalutamide is associated with prostate tumour progression in a new model system. *Br J Cancer* 81(2):242–251.
22. Nguyen TV, Yao M, Pike CJ (2007) Flutamide and cyproterone acetate exert agonist effects: Induction of androgen receptor-dependent neuroprotection. *Endocrinology* 148(6):2936–2943.
23. Huggins C, Hodges CV (2002) Studies on prostatic cancer. I. The effect of castration, of estrogen and of androgen injection on serum phosphatases in metastatic carcinoma of the prostate. 1941. *J Urol* 167(2 Pt 2):948–951, discussion 952.
24. Semenas J, Dizeyi N, Persson JL (2013) Enzalutamide as a second generation antiandrogen for treatment of advanced prostate cancer. *Drug Des Devel Ther* 7:875–881.
25. Huggins C (1963) The hormone-dependent cancers. *JAMA* 186(5):481–483.
26. Koivisto P, et al. (1997) Androgen receptor gene amplification: A possible molecular mechanism for androgen deprivation therapy failure in prostate cancer. *Cancer Res* 57(2):314–319.
27. Stanbrough M, et al. (2006) Increased expression of genes converting adrenal androgens to testosterone in androgen-independent prostate cancer. *Cancer Res* 66(5):2815–2825.
28. Montgomery RB, et al. (2008) Maintenance of intratumoral androgens in metastatic prostate cancer: A mechanism for castration-resistant tumor growth. *Cancer Res* 68(11):4447–4454.
29. Sasaki J, et al. (2005) Regulation of anaphylactic responses by phosphatidylinositol phosphate kinase type I alpha. *J Exp Med* 201(6):859–870.
30. Hasegawa H, et al. (2012) Phosphatidylinositol 4-phosphate 5-kinase is indispensable for mouse spermatogenesis. *Biol Reprod* 86(5):136, 1–12.
31. Yamaguchi H, et al. (2010) Phosphatidylinositol 4,5-bisphosphate and PIP5-kinase Ialpha are required for invadopodia formation in human breast cancer cells. *Cancer Sci* 101(7):1632–1638.
32. Larsson R, Blanco N, Johansson M, Sterner O (2012) Synthesis of C-1 indol-3-yl substituted tetrahydroisoquinoline derivatives via a Pictet–Spengler approach. *Tetrahedron Lett* 53(37):4966–4970.
33. Goldstein DM, Gray NS, Zarrinkar PP (2008) High-throughput kinase profiling as a platform for drug discovery. *Nat Rev Drug Discov* 7(5):391–397.
34. Merkle D, Hoffmann R (2011) Roles of cAMP and cAMP-dependent protein kinase in the progression of prostate cancer: Cross-talk with the androgen receptor. *Cell Signal* 23(3):507–515.
35. Taylor BS, et al. (2010) Integrative genomic profiling of human prostate cancer. *Cancer Cell* 18(1):11–22.
36. Dienstmann R, Rodon J, Markman B, Tabernero J (2011) Recent developments in anticancer agents targeting PI3K, Akt and mTORC1/2. *Recent Patents Anticancer Drug Discov* 6(2):210–236.
37. Deep G, Oberlies NH, Kroll DJ, Agarwal R (2008) Isosilybin B causes androgen receptor degradation in human prostate carcinoma cells via PI3K-Akt-Mdm2-mediated pathway. *Oncogene* 27(28):3986–3998.
38. Carver BS, et al. (2011) Reciprocal feedback regulation of PI3K and androgen receptor signaling in PTEN-deficient prostate cancer. *Cancer Cell* 19(5):575–586.
39. Mulholland DJ, et al. (2011) Cell autonomous role of PTEN in regulating castration-resistant prostate cancer growth. *Cancer Cell* 19(6):792–804.
40. Chen S, Xu Y, Yuan X, Bubley GJ, Balk SP (2006) Androgen receptor phosphorylation and stabilization in prostate cancer by cyclin-dependent kinase 1. *Proc Natl Acad Sci USA* 103(43):15969–15974.